Propellants, Explosives, Pyrotechnics

Propellants, Explosives, Pyrotechnics

RESEARCH ARTICLE OPEN ACCESS

Condensing the Cage: Novel Insights Into the Reaction Pathway of Isowurtzitane Cage Formation

Campbell S. Wolfe[1] | Patrick F. N. Stewart[2] | Rory M. Campbell[2] | James R. White[2] | Alison M. Beardah[2] | Justin Fellows[2] | Thomas Wirth[1]

[1]School of Chemistry, Cardiff University, Cardiff Cymru, UK | [2]Defence Science and Technology Laboratory (DSTL), Salisbury, Wiltshire, UK

Correspondence: Thomas Wirth (wirth@cf.ac.uk)

Received: 17 April 2026 | **Revised:** 19 August 2026 | **Accepted:** 24 August 2026

Keywords: CL-20 | energetic materials | HRMS | isowurtzitane cages | mechanistic investigations

ABSTRACT

In this contribution, we propose an alternative reaction pathway for the formation of isowurtzitane cages. These cage products are the basis for the synthesis of CL-20, a highly prized energetic material and propellant. Isowurtzitane cages are typically formed under acid-catalysed conditions via the condensation reaction between glyoxal and certain amines. Here, we report the cage formation proceeds *via* a series of addition reactions from the previously established diimine intermediate. This reaction pathway has been investigated in detail with HRMS and NMR, as well as isolation of key intermediates providing a comprehensive alternative pathway for the cage formation.

1 | Introduction

CL-20 **1** (Figure 1), also known as HNIW, is one of the most powerful secondary explosives currently known. It has superior detonation velocity and higher crystal density than RDX, which is currently the most common energetic material in the defence industry (CL-20: 9500 m s^{-1} and 2.04 g cm^{-1} in the ε polymorph vs. RDX: 8750 m s^{-1} and 1.81 g cm^{-1}) [1]. Due to its favourable characteristics as a propellant, it is highly valuable to further understand the formation of this cage molecule and to provide room for synthetic exploration [1, 2].

Typically, CL-20 **1** is synthesised *via* the polycyclic isowurtzitane cage HBIW **4** as reported by Nielsen et al. (Scheme 1) [3]. Following the formation of the isowurtzitane cage structure, the benzyl groups are replaced with acetyl groups *via* a palladium catalysed hydrogenation in the presence of acetic anhydride, to form TADBIW **5**, which is then nitrated [4].

The nitration has been performed by various methods; $NOBF_4/NO_2BF_4$ [4], mixed acid media [5], HNO_3/N_2O_5 [6], oxidation using cerium(IV) ammonium nitrate (CAN) [7], ionic liquids [8], or a zeolite/HNO_3 system [9]. Much of the synthetic work on isowurtzitane cage synthesis has focused on optimising reaction conditions where different acids [10, 11], catalysts [12, 13], solvents [10, 11, 14], and amines [11], have been investigated.

Another well-studied area of synthetic research is the preparation of isowurtzitane cage structures beyond compound **5**. These synthetic routes provide further ways to access CL-20 **1** by avoiding toxic by-products (TAIW **8** [15]), utilising cheaper materials (HAIW **7** [7, 16], and HSIW **10** [17]) or improving reaction rates (TADF **9** [18, 19]) as shown in Figure 2.

Abbreviations: CAN, Cerium(IV) ammonium nitrate; HAIW, Hexaacetylisowurtzitane; HBIW, Hexabenzylisowurtzitane; HRMS, High resolution mass spectrometry; HSIW, Hexasulfonylisowurtzitane; NCIs, Non-covalent Interactions; N.D., Not detected; NMR, Nuclear magnetic resonance; TADBIW, Tetraacetyldibenzylisowurtzitane; TADF, Tetraacetyldiformylisowurtzitane; TAIW, Tetraacetylisowurtzitane; TOF, Time of flight analyser.

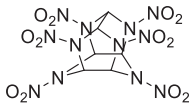

CL-20 **1**

FIGURE 1 | CL-20 **1**.

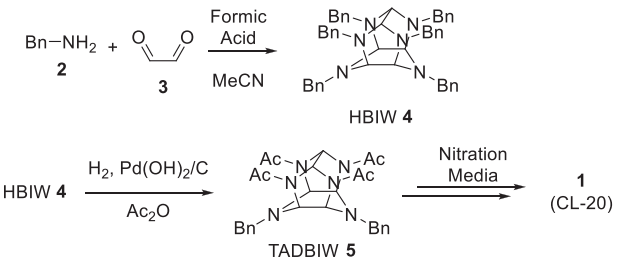

SCHEME 1 | Reported synthesis of CL-20 **1** from benzylamine **2** and glyoxal **3**.

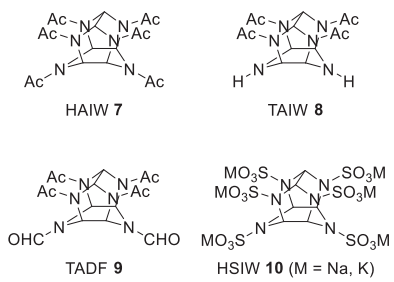

FIGURE 2 | Some reported modifications of isowurtzitane cage investigated as precursors to CL-20 **1**.

In the original publication, Nielsen et al. suggested an initial formation of diimine **11** from glyoxal **3** and benzylamine **2** [3], which is in-line with known amine condensations [20].

As glyoxal **3** is commercially available and typically used as an aqueous 40% solution, the role of water in the reaction conditions is worth considering. Scheme 2 depicts a plausible six-membered transition state and provides a theoretical role of water in the reaction system. Compound **11a** may also be formed during the reaction (Scheme 2) [20–22].

Nielsen et al. reported that diimine **11** reacts with itself in a trimerisation sequence [3]. They propose a series of intermediates

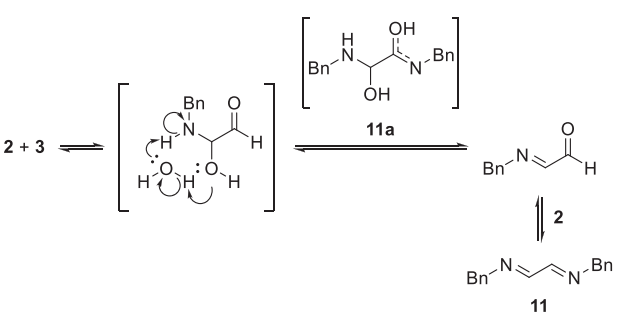

SCHEME 2 | Formation of diimine **11** from benzylamine **2** and glyoxal **3**.

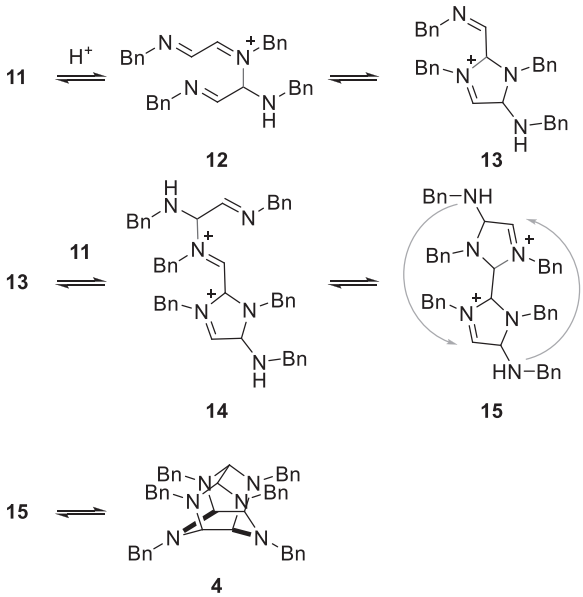

SCHEME 3 | Formation mechanism of isowurtzitane structure as proposed by Nielsen et al. [3].

starting with a dimerisation of **11** to form **12** under acidic conditions and subsequent ring closure to **13**. Another molecule **11** is added to generate **14**, which undergoes ring closure to produce the bicyclic intermediate **15**. After a conformational change (not shown), the two secondary amine moieties undergo further ring closure at the remaining iminium positions, to give the final isowurtzitane cage structure **4**. The two bonds formed in the final cyclisation to give the six-membered ring are indicated by arrows in **15** and are highlighted in bold in **4** (Scheme 3).

To support this mechanistic proposal, Nielsen reported the isolation of two key intermediates. Firstly, a dihemiaminal **11a** resulting from the addition of two benzylamine **2** molecules to glyoxal **3** and, secondly, the diimine **11** (Scheme 2, see above). Nielsen achieved their synthesis and isolation by changing the reaction conditions to a more polar solvent system, causing **11** to precipitate prior to forming product **4** [3]. Nielsen subsequently reported that the isolated diimine **11** can react under the reaction conditions to produce the desired isowurtzitane cage structure HBIW **4** [3]. This work has stood as the standard mechanism of this reaction for over 30 years, and little further synthetic work has been undertaken since.

In addition to the synthetic work surrounding isowurtzitane cage formation, computational studies have examined various aspects of the mechanism. In 2017, Dong et al. investigated the formation of the dihemiaminal **11a** via DFT studies and reported that the formation of the diimine **11** requires acid for the elimination of water to be favourable. They report a calculated energy barrier of 217.6 and 253.1 kJ mol^{-1} for each water elimination step without acid, respectively. This is clearly unfavourable in comparison to their calculated energy barrier of 71.6 kJ mol^{-1} for the same reaction with acid [23].

By comparing the energy barriers of three amines, Shang et al. suggested that the π–π stacking effect produced by benzylamine has a favourable effect on the isowurtzitane cage formation. They

reported that for their proposed rate-determining step, benzylamine has the lowest energy barrier of 82.0 kJ mol^{-1}, allylamine an energy barrier of 88.7 kJ mol^{-1}, and methylamine (which has not been used in a successful cage formation experimentally) had a theoretical energy barrier of 92.9 kJ mol^{-1}. They hypothesise this decrease in energy barrier is due to the ability of the benzene rings to coordinate with each other due to non-covalent interactions (NCI's) between the π-systems [24, 25].

Preceding the rate determining step, Shang proposes that the bicyclic intermediate **15** could form different rotational isomers, due to the four chiral centres present in the proposed structure. It was concluded that two of the fourteen possible structures (there are two *meso*-compounds) are feasible for the cyclisation step. Shang reported a calculated 10.9 kJ mol^{-1} difference between investigated cages. This difference is too small to fully account for the fact that methylamine cannot form the cage experimentally, but both allyl- and benzylamine can. The energy barriers corresponding to this investigation of chirality were used explain the experimental observations and also highlights the importance of the chirality for these intermediates (see the Supporting Information for an exhaustive list of intermediates **15**).

In this work, through NMR and HRMS studies, we describe evidence for an alternative reaction pathway, starting from the same diimine intermediate **11**. This alternative pathway can act as inspiration for future authors to tackle alternative isowurtzitane synthesis. These could include further improvements of existing routes or all together novel routes which could even bypass the challenging palladium catalysed step.

2 | Experimental Section

For this work, 'standard reaction conditions' refer to the use of benzylamine **2** and glyoxal **3** in a ratio of 2.2:1 under formic acid catalysed conditions, at room temperature for 24 h. All high-resolution mass spectra discussed were obtained from Cardiff University on a Waters GC-TOF spectrometer or Water LCT premier XE spectrometer. Ions were generated using electron ionisation (EI) or electrospray ionisation (ES). All signals are reported as a mass-to-charge ratio (m/z). For a full list of the experimental protocols, see Supporting Information.

3 | Results and Discussion

3.1 | Diimine Isolation

Nielsen reported the isolation of the diimine **11** using reaction conditions modified from the original synthesis. Utilising a more polar solvent mixture H_2O:EtOH in a 1:1 ratio, should cause the diimine **11** to precipitate prior to forming the cage product. However, it was found that cage products could be detected by NMR and HRMS analysis. Isolation of the diimine **11** proved more challenging than expected. Even with conditions that should be very unfavourable for cage formation, the NMR showed characteristic signals for HBIW **4** around the 4–4.2 ppm region matching the reported values [3].

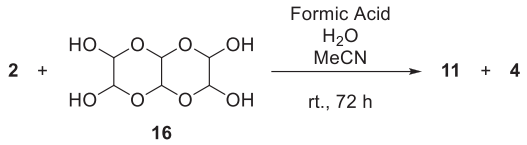

SCHEME 4 | Use of glyoxal trimer dihydrate **16** under standard reaction conditions for 72 h.

Different reaction conditions for diimine **11** formation were investigated (see Supporting Information), but the HRMS signal for HBIW **4** was consistently present. Careful examination of starting materials showed no contamination. The hypothesis to explain the rapid cage formation is in line with the work of Shang et al. In their work, they conclude that the rate determining step of the cage formation is complex including the formation of many possible stereoisomers. Thus, if the correct stereoisomers are energetically favoured, they could form quickly. This suggests that the extended reaction time (up to 24 h) arises from the formation of unfavourable conformers, which must surmount the reverse activation energy barrier to revert to intermediates capable of re-forming the favoured stereochemistry [24, 25].

It was necessary to find a procedure which could reliably form the diimine **11** without also forming cage **4**, so alternative starting materials were investigated. It has been reported that glyoxal favourably forms its mono- and di-acetal-hydrates in aqueous conditions. Additionally, glyoxal oligomerises to its stable trimer dihydrate **16** under acidic conditions [26, 27].

When **16** was reacted under the standard reaction conditions (for 72 h) an inseparable mixture of **11** and **4** was formed, this indicates the reaction is much slower in comparison to aqueous glyoxal (Scheme 4).

The reaction was monitored *in situ via* NMR and compound **11** was detected immediately and compound **4** was not detected until after 30 min of reaction time had elapsed. This provided a window wherein diimine **11** could be isolated separately from HBIW **4**. This monitoring was extended over a period of 72 h *via* NMR; however, there were too many overlapping signals to obtain meaningful quantitative data.

This window was utilised to directly synthesise the diimine **11** with a shortened reaction time and use of **16** as a starting material.

3.2 | Cage Formation From Diimine

Compound **11** was exposed to the standard reaction conditions described by Nielsen et al. [3], in the absence of benzylamine **2**. However, compound **4** could not be detected by HRMS. When the reaction was repeated in the presence of benzylamine **2**, a new species, compound **17**, was detected (Scheme 5).

This compound **17** suggests that diimine **11** is reactive towards amines and with this new perspective we were able to explore a different angle to the cage formation *via* HRMS.

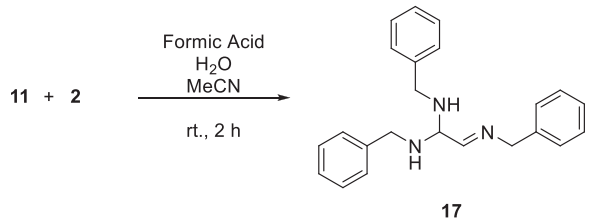

SCHEME 5 | Reaction between diamine **11** and benzylamine **2**.

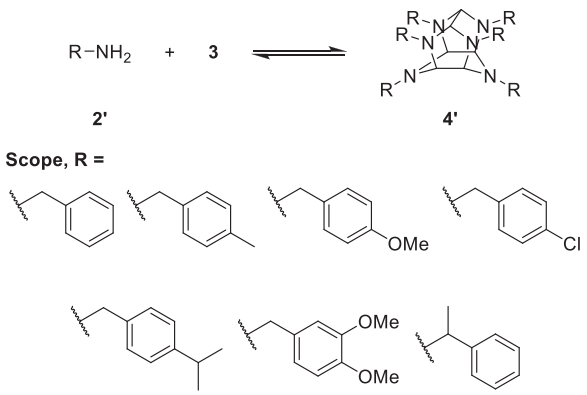

SCHEME 6 | Benzylamine derivatives **2'** monitored by HRMS, x-ray structures have been obtained for **4** and **4'** (R = 4-Me-C_6H_4-CH_2-) [29].

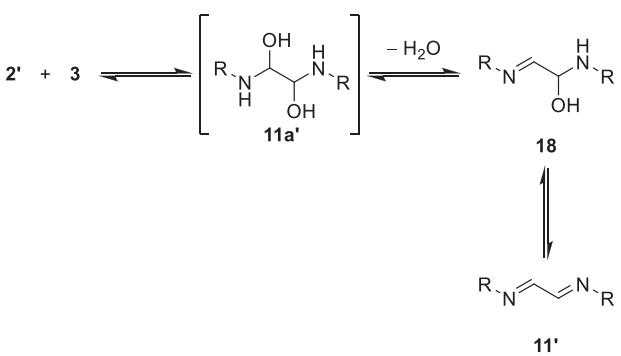

SCHEME 7 | Formation of diimine **11**, brackets: N.D.

3.3 | A New Pathway: Conclusions From HRMS

The reaction was monitored *via* HRMS utilising a scope of seven benzylamine derivatives under the standard reaction conditions and samples were taken after 2 h to monitor for corresponding *(m/z)* signals across multiple spectra. In all cases reported species have at least two corresponding signals, most species have MS signals in all spectra (for full spectra breakdown see Supporting Information) (Scheme 6).

The alternative pathway starts with the previously reported diimine **11'** formation (Scheme 7).

The hemiaminal **11a'** that Nielsen et al. reports was not detected by HRMS; however, Nielsen also reports that this product eliminates water to give **11'** under low pressure conditions [3]. Thus, it is possible that the reduced pressure conditions of the TOF detector in MS could cause this elimination, thereby rendering the parent ion undetectable [28].

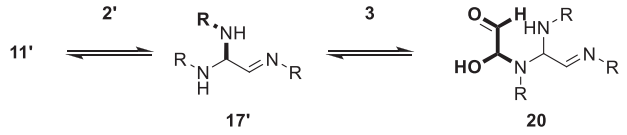

SCHEME 8 | Subsequent reaction of diimine **11** to **20**.

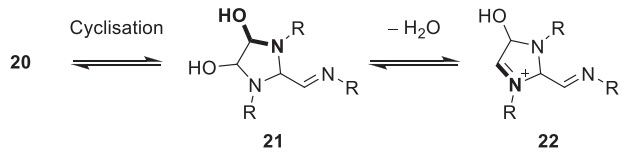

SCHEME 9 | Pathway from **20** to **22**.

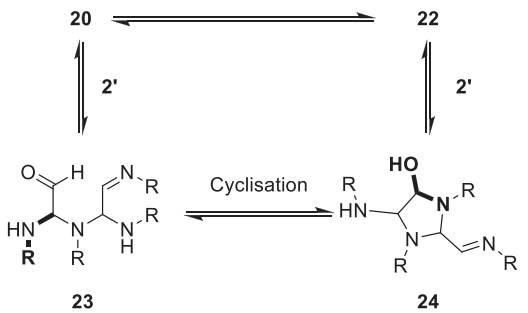

SCHEME 10 | Branching pathway from **20**.

The addition of **2'** to **11'** gives **17'**, as previously discussed, followed by addition of another moiety of **3** to form a new compound **20** (Scheme 8).

Here, a diversion in the reaction pathway is suggested. These are likely competing pathways, and each contributes to the overall picture from the HRMS data, so they are considered separately. The pathways have been assigned Pathway A: The imine route and Pathway B: The hemiaminal route.

3.3.1 | Pathway A: The Imine Route

In pathway A, the imine moiety is preserved throughout most of the reaction. This moiety is likely in equilibria with the corresponding hemiaminal [20], but it is represented as an imine here for clarity.

Intermediate **20** can undergo a cyclisation to **21** and water elimination to **22** (Scheme 9).

It should be noted that one limitation of this heavy reliance on HRMS is that iminium ions exist in equilibria with their enamine counterparts, and these species cannot be differentiated by HRMS, due to equivalent chemical formulae of the ions (enamine as $[M + H]^+$, iminium as $[M]^+$) [20].

Subsequently, **20** can undergo multiple reactions. The previously discussed route to **22** allows direct access to **24** upon the addition of **2'**, or **20** can first react directly with another equivalent of amine **2'** to give **23** which can then cyclise to **24**. As both **23** and **24** are detected, the pathways are likely in competition (Scheme 10).

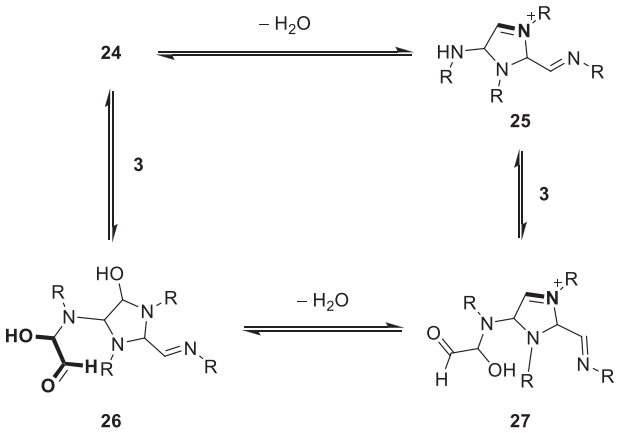

SCHEME 11 | Branching pathway from **24**.

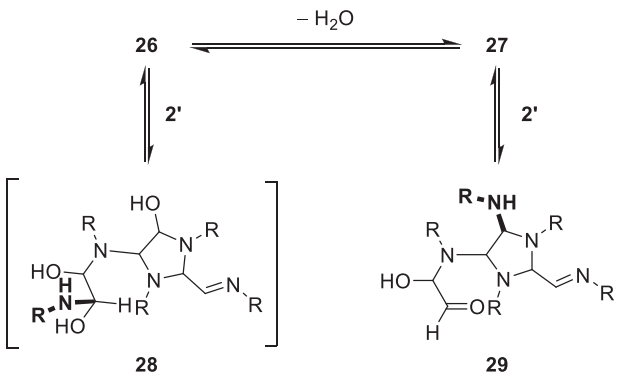

SCHEME 12 | Branching pathway from **26**. Brackets: N.D.

Either route furnishes compound **24**, which can either eliminate water to give compound **25** or directly react with an equivalent of glyoxal **3** to give compound **26**. In either case, the formation of species **27** proceeds from either **26** or **25** (Scheme 11).

Whilst intermediates **26** and **27** are in equilibria, they retain the branched pathway as both are able to react with an equivalent of amine **2'** to give compounds **28** and **29**, respectively (Scheme 12).

It should be noted that compound **28** is not directly observed, however, due to the presence of 3 hemiaminal groups, it is possible that, similar to how Neilsen et al. describes hemiaminal **11'** (see above), it is not possible to detect such a parent ion *via* MS due to the reduced pressure of a TOF analyser. Compound **28** is still proposed as a logical step in the synthesis due to the surrounding evidence, although it does highlight a challenge with this method of reaction monitoring.

The branching pathway can reunite *via* forming of **30** from **28** and **31** from **29**, respectively, and give the equilibria between these species (Scheme 13).

Intermediate **31** is also capable of undergoing a divergent pathway, if compound **31** is directly attacked by amine **2'** compound **32** is formed, followed by compound **33**. If water elimination occurs first, to give compound **34**, this is attacked by **2'** to give **35**. Here, the amine moiety is substituted directly on the six-membered

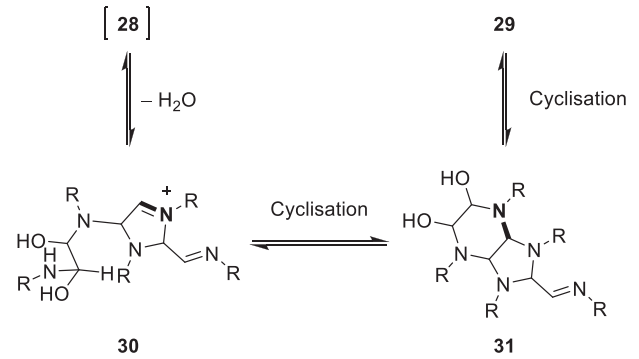

SCHEME 13 | Compounds **30** and **31** in equilibria with compounds **28** and **29**.

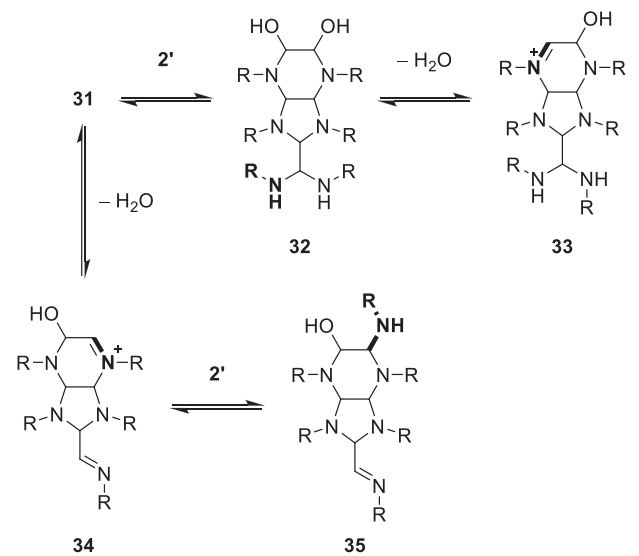

SCHEME 14 | Branching pathway from compound **31**.

ring, as opposed to an attack at the imine, as in compound **33** (Scheme 14).

Finally, **33** and **35** converge to give two alternative penultimate intermediates, **36** and **37**, respectively. These intermediates are chemically equivalent; the only difference is which bond is formed in the penultimate step. Both of these bonds are part of the five membered rings, the formation of the bond in the six-membered ring as the last intermediate is explored in pathway B. These intermediates both undergo elimination of water to give **38** which can complete the final intermolecular cyclisation to give cage **4'** (Scheme 15).

3.3.2 | Pathway B: The Hemiaminal Route

Pathway B is characterised by the preservation of the branched hemiaminal moiety, after the formation of **11'**, giving **39**. Inevitably, these two species are in equilibria with each other, but as there are often signals in the MS corresponding to both species, and some alternative chemistry can be demonstrated by treating them separately, they are shown as such (Scheme 16).

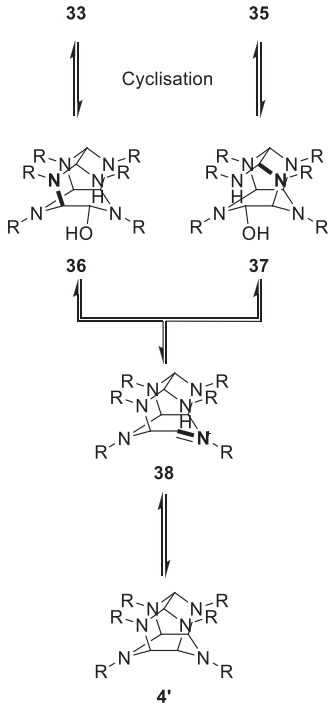

SCHEME 15 | Cage **4'** formation from pathway A.

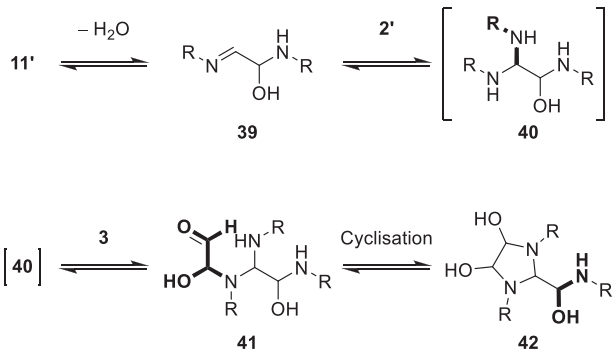

SCHEME 16 | Pathway B splits from **11'**, giving **39**, **41**, and **42**, possibly *via* **40**. Brackets: N.D.

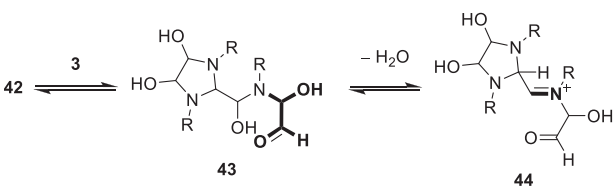

SCHEME 17 | Compound **42** reacts with **3** to give **43**, and then **44** *via* water elimination.

Intermediate **42** can cyclise from **41** if the pathway proceeds *via* **40**, an intermediate which was not observed by MS. However, intermediate **40** is suggested as a logical follow though for the formation of **41** as it explains otherwise unattributed MS signals. The masses of **42** (Scheme 16, see above) and **43**, **44**, **45**, and **46**, see below (Scheme 17 and 18), are explained exclusively by pathway B. Compound **42** is able to attack glyoxal **3** to give **43**, which can eliminate water to give the corresponding iminium **44** (Scheme 17).

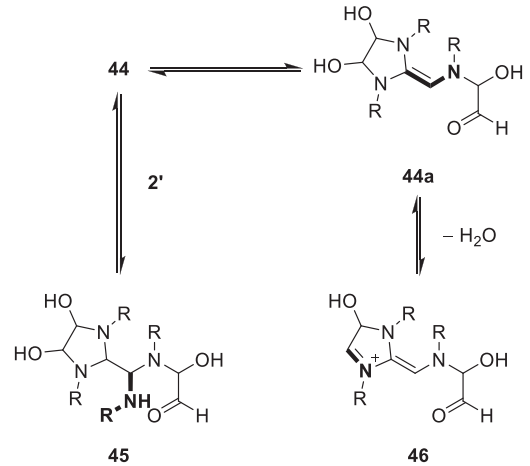

SCHEME 18 | Compound **44** forms enamine **44a** or reacts with **2'** to give **45**.

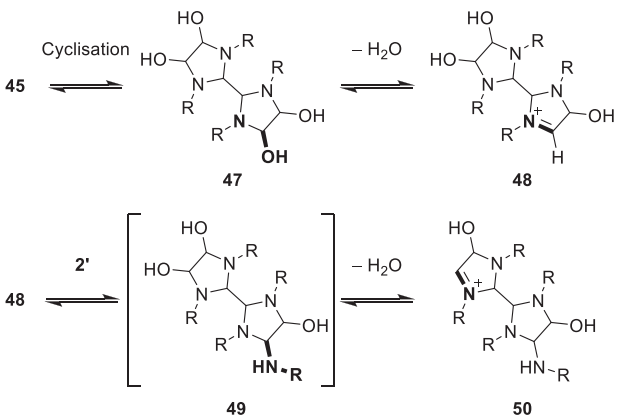

SCHEME 19 | Compound **45** undergoes a cyclisation to **47** and eventually **50** *via* two eliminations of H_2O and an addition of **2'**.

Following formation of **44**, there is a potential branch in the pathway. Compound **44** can react with **2'** to give **45** or can form the enamine **44a** and eliminate water to give **46**. The formation of the enamine explains why the corresponding $[M]^{2+}$ ions for subsequent intermediates are not observed but the masses for the $[M]^{+}$ ions are (Scheme 18).

The branches from compound **44** are shown separately, starting with the formation of **45**. This cyclisation gives **47**, followed by water elimination to **48**. This iminium can react with **2'**, however, intermediate **49** is not directly observed, only the corresponding elimination product **50**. As before there are three readily eliminated hemiaminal moieties, so the non-detection of **49** is not wholly surprising (Scheme 19).

The next step in this part of this route is an addition of **2'** to **50** to give **51**, followed by water elimination to **52** (Scheme 20).

Compound **52** leads to the penultimate step in this route, which will be considered in tandem with the other branch, first mentioned in Scheme 17 (see above). Thus, the alternative route proceeding from compound **46** is shown (Scheme 21).

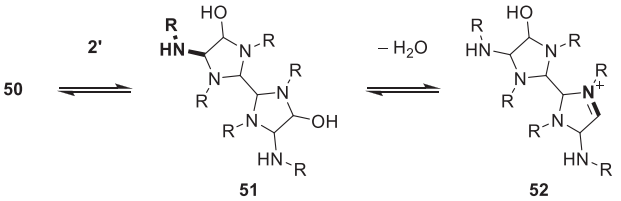

SCHEME 20 | Compound **50** forms **52** *via* **51**.

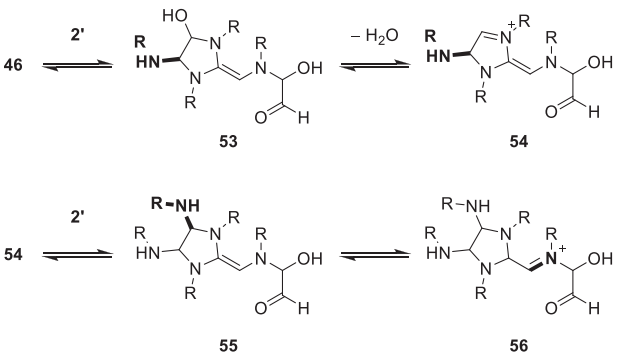

SCHEME 21 | Pathway branch from **46** gives **56** *via* two additions of **2'** and an elimination of H_2O.

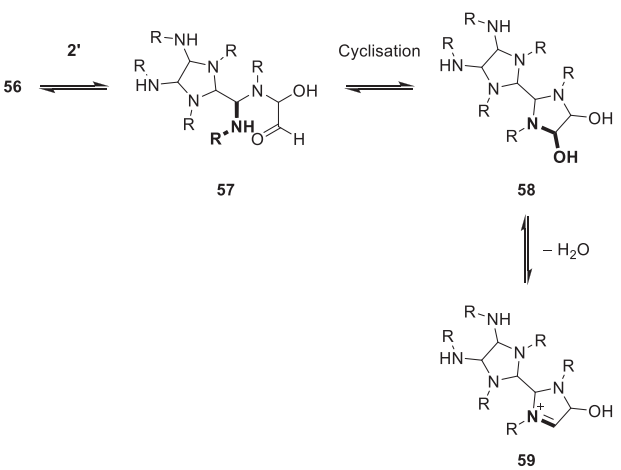

SCHEME 22 | Formation of **59** from **56** *via* **57** and **58**.

In Scheme 21, the formation of compound **53** *via* an addition of **2'** is shown. Subsequent water elimination, followed by further addition of **2'** gives compounds **54** and **55**, respectively. At this point, the charge that was otherwise present on the five-membered ring has been neutralised and so the iminium position as shown in compound **56** can be reconsidered.

Following the formation of compound **56**, an addition of **2'** to give **57** can occur. This is the same substitution that took place in the formation of **45** from **44**, enabling cyclisation to **58** and elimination to give **59** (Scheme 22).

Finally, the branches reunite as **52** and **59** cyclise to give the same compound **60**. This acts in a similar manner as the penultimate step of pathway A, where water is eliminated to give **61** and the final intermolecular reaction gives the cage **4'** (Scheme 23).

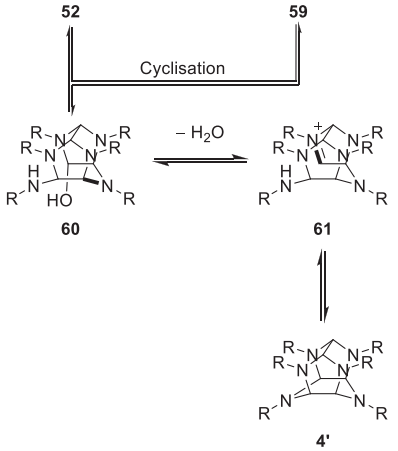

SCHEME 23 | Cage **4'** formation *via* pathway B.

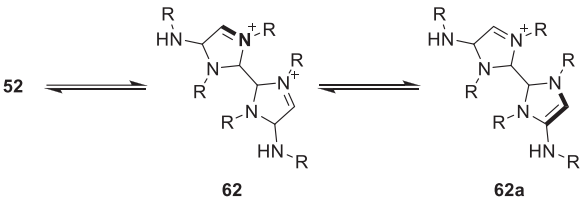

SCHEME 24 | $[M]^{+2}$ species **62**, and corresponding enamine **62a**.

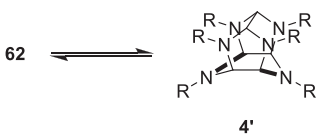

SCHEME 25 | Cage **4'** formation from compound **62**.

One last consideration for pathway B is an alternative order of the final steps. Instead of cyclising to **60**, **52** can eliminate another equivalent of water to give the doubly charged species **62**, which was observed as an $[M]^{2+}$, this species is identical to the final intermediate proposed by Nielsen et al. (Scheme 24) [3].

Lastly, this alternative intermediate, **62** can ring close at both iminium positions to give the cage **4'** (Scheme 25).

With this, an extensive alternative reaction pathway is shown for the formation of the isowurtzitane cage HBIW **4** and several of its derivatives. HRMS is used as the primary technique to explore this complex array of plausible species (time delayed NMR is presented in the Supporting Information) and whilst this methodology does have the limitation of not being able to distinguish between alternative suggestions for the same chemical isotope, it offers unprecedented means to explore the otherwise unnavigable branches of this synthesis.

4 | Conclusion

An extensive alternative reaction pathway for the formation of isowurtzitane cages is shown and the evidence for this *via* HRMS and NMR is explored. The NMR data shows a clear signal for a rapidly forming imine species, in-line with the literature-reported

diimine **11**. The NMR study shows that benzylamine **2** and glyoxal **3** readily form some amount of cage **4**, even under synthetically unfavourable conditions. This NMR observation in conjunction with HRMS showed that the reaction of benzylamine **2** with glyoxal trimer **16** was sufficiently slow to allow proper isolation of the diimine intermediate **11**. This was exploited to uncover evidence of a complex alternative pathway to cage formation.

The alternative pathway is intricate and contains multiple branching pathways in competition with each other, hence HRMS was the most suitable means to explore this chemical space. This does have a limitation, in that multiple plausible suggestions for the same chemical isotope signal are indistinguishable. To alleviate this a small substrate scope of benzylamine derivatives to relate multiple corresponding HRMS signals for equivalent structures was explored.

We hope this work can serve as the basis for future synthetic exploration of this multi-faceted reaction and aid other authors in exploring this chemical space.

Furthermore, the greater understanding of the complexities of this cage formation will enable authors to envision brand new synthetic pathways, potentially even bypassing the troublesome palladium catalysis step.

Acknowledgements

We would like to thank Cardiff University for the facilities and laboratory space, and we would particularly like to thank Peter Iafrate and Simon Waller for their extensive help with the MS data processing, which formed the cornerstone of this work. We thank DSTL for both the funding and their continued support throughout this project. We also thank Dr. Benson M. Kariuki and the UK National Crystallography Service, Southampton, for obtaining x-ray data.

Conflicts of Interest

The authors declare no conflicts of interest.

Data Availability Statement

The data that supports the findings of this study are available in the Supporting Information of this article.

References

1. T. M. Klapötke, *Chemistry of High-Energy Materials* (De Gruyter, 2019).

2. A. K. Sider, N. Sikder, B. R. Gandhe, J. P. Agrawal, and H. Singh, "Hexanitrohexaaza-Isowurtzitane or CL-20 in India: Synthesis and Characterisation," *Defence Science Journal* 52, no. 2 (2002): 135–146, https://doi.org/10.14429/dsj.52.2158.

3. A. T. Nielsen, R. A. Nissan, D. J. Vanderah, C. L. Loon, R. D. Gilardi, C. F. George, and J. Flippen-Anderson, "Polyazapolycyclics by Condensation of Aldehydes With Amines," *Journal of Organic Chemistry* 55 (1990): 1459–1466, https://doi.org/10.1021/jo00292a015.

4. A. T. Nielsen, A. P. Chafin, S. L. Christian, et al., "Synthesis of Polyazapolycyclic Caged Polynitramines," *Tetrahedron* 54, no. 39 (1998): 11793–11812, https://doi.org/10.1016/S0040-4020(98)83040-8.

5. N. V. Latypov, U. Wellmar, P. Goede, and A. J. Bellamy, "Synthesis and Scale-Up of 2,4,6,8,10,12-Hexanitro-2,4,6,8,10,12-hexaaza-isowurtzitane From 2,6,8,12-Tetraacetyl-4,10-dibenzyl-2,4,6,8,10,12-hexaazaisowurtzitane (HNIW, CL-20)," *Organic Process Research & Development* 4, no. 3 (2000): 156–158, https://doi.org/10.1021/op990097d.

6. Y. Bayat and F. Hajighasemali, "An Efficient and Facile Synthesis of CL-20 From TADNO Using HNO_3/N_2O_5 and Optimization of Reaction Parameters by Taguchi Method," *Propellants, Explosives, Pyrotechnics* 41, no. 5 (2016): 893–898, https://doi.org/10.1002/prep.201500347.

7. G. M. Gore, R. Sivabalan, U. R. Nair, A. Saikia, S. Venugopalan, and B. R. Gandhe, "Synthesis of CL-20 (IV) by Oxidative Debenzylation with Cerium(IV) Ammonium Nitrate (CAN)," *ChemInform* 38, no. 29 (2007), https://doi.org/10.1002/chin.200729147.

8. Y. Bayat, M. M. Ahari-Mostafavi, and N. Hasani, "[Hmim][HSO_4], a Green and Recyclable Acidic Ionic Liquid Medium for the One-Pot Nitration of TADB to HNIW," *Propellants, Explosives, Pyrotechnics* 39, no. 5 (2014): 649–652, https://doi.org/10.1002/prep.201300153.

9. Y. Bayat, F. Hajighasemali, and A. Mohajeri, "Synthesis of CL-20 From TADB in a One-Pot Method by Zeolite/HNO_3 as a New Nitrolysis System," *Journal of the Brazilian Chemical Society* 27, no. 6 (2016): 1103–1108.

10. T. Gołofit and P. Maksimowski, "Purification of Hexabenzylhexaazaisowurtzitane," *Central European Journal of Energetic Materials* 13 (2016): 1038–1050.

11. G. Herve, G. Jacob, and R. Gallo, "Preparation and Structure of Novel Hexaazaisowurtzitane Cages," *Chemistry—A European Journal* 12, no. 12 (2006): 3339–3344, https://doi.org/10.1002/chem.200501032.

12. J. V. Viswanath, K. J. Venugopal, N. V. S. Rao, and A. Venkataraman, "An Overview on Importance, Synthetic Strategies and Studies of 2,4,6,8,10,12-Hexanitro-2,4,6,8,10,12-hexaazaisowurtzitane (HNIW)," *Defence Technology* 12, no. 5 (2016): 401–418, https://doi.org/10.1016/j.dt.2016.05.002.

13. V. Azizkhani, F. Montazeri, E. Molashahi, and A. Ramazani, "Magnetically Recyclable $CuFe_2O_4$ Nanoparticles as an Efficient and Reusable Catalyst for the Green Synthesis of 2,4,6,8,10,12-Hexabenzyl-2,4,6,8,10,12-hexaazaisowurtzitane as CL-20 Explosive Precursor," *Journal of Energetic Materials* 35, no. 3 (2017): 314–320, https://doi.org/10.1080/07370652.2016.1190795.

14. Y. A. Kryukov, I. A. Surmacheva, and S. V. Sysolyatin, "Effect of Physicochemical Properties of the Solvent on Synthesis of Dodecane Derivatives," *Khimi Tekhnol* 12, no. 1 (2011): 14–19.

15. K. Dong, C. H. Sun, J. W. Song, G. X. Wei, and S. P. Pang, "Synthesis of 2,6,8,12-Tetraacetyl-2,4,6,8,10,12-hexaazaisowurtzitane (TAIW) From 2,6,8,12-Tetraacetyl-4,10-dibenzyl-2,4,6,8,10,12-hexaazaisowurtzitane (TADBIW) by Catalytic Hydrogenolysis Using a Continuous Flow Process," *Organic Process Research & Development* 18, no. 11 (2014): 1321–1325, https://doi.org/10.1021/op500020d.

16. A. Ramazani, V. Azizkhani, and S. W. Joo, "Heteropolyacids: As Efficient Catalysts for the Nitration of 2,4,6,8,10,12-Hexaacetyl-2,4,6,8,10,12-hexaazaisowurtzitane," *Revue Roumaine de Chimie* 64, no. 7 (2019): 569–575, https://doi.org/10.33224/rrch/2019.64.7.03.

17. S. V. Sysolyatin, G. V. Sakovich, and V. N. Surmachev, "Methods for the Synthesis of Polycyclic Nitramines," *Russian Chemical Reviews* 76, no. 7 (2007): 673–680, https://doi.org/10.1070/RC2007v076n07ABEH003716.

18. S. Jin, Q. Shu, S. Chen, and Y. Shi, "Preparation of ε-HNIW by a One-Pot Method in Concentrated Nitric Acid From Tetraacetyldiformylhexaazaisowurtzitane," *Propellants, Explosives, Pyrotechnics* 32, no. 6 (2007): 468–471, https://doi.org/10.1002/prep.200700053.

19. S. V. Sysolyatin, A. A. Lobanova, Y. T. Chernikova, and G. V. Sakovich, "Methods of Synthesis and Properties of Hexanitrohexaazaisowurtzitane," *Russian Chemical Reviews* 74, no. 8 (2005): 757–764, https://doi.org/10.1070/RC2005v074n08ABEH001179.

20. R. W. Layer, "The Chemistry of Imines," *Chemical Reviews* 63, no. 5 (1963): 489–510, https://doi.org/10.1021/cr60225a003.

21. E. H. Cordes and W. P. Jencks, "The Mechanism of Hydrolysis of Schiff Bases Derived From Aliphatic Amines," *Journal of the American Chemical Society* 85, no. 18 (1963): 2843–2848, https://doi.org/10.1021/ja00901a037.

22. Y. Valadbeigi and H. Farrokhpour, "Simple and Water-Assisted Tautomerism in Succinimide," *Structural Chemistry* 26, no. 2 (2015): 539–545, https://doi.org/10.1007/s11224-014-0511-6.

23. K. Dong, C.-H. Sun, S.-W. Zhang, H.-Y. Wang, J.-W. Song, and S.-P. Pang, "Condensation Mechanism of Cage Hexabenzylhexaazaisowurtzitane From Glyoxal and Benzylamine: A Computational Study," *New Journal of Chemistry* 41, no. 21 (2017): 12694–12699, https://doi.org/10.1039/C7NJ00972K.

24. F. Shang, R. Liu, M. Lv, and Y. Ma, "Unraveling the Key Role of the Benzyl Group in the Synthesis of CL-20 Precursor HBIW," *ACS Omega* 7, no. 25 (2022): 21912–21924, https://doi.org/10.1021/acsomega.2c02161.

25. M. J. Rashkin and M. L. Waters, "Unexpected Substituent Effects in Offset π–π Stacked Interactions in Water," *Journal of the American Chemical Society* 124, no. 9 (2002): 1860–1861, https://doi.org/10.1021/ja016508z.

26. P.-R. Chen and L.-K. Chu, "Infrared Characterization of Hydrated Products of Glyoxal in Aqueous Solution," *Spectrochimica Acta Part A: Molecular and Biomolecular Spectroscopy* 306 (2024): 123571, https://doi.org/10.1016/j.saa.2023.123571.

27. J. Liggio, S. M. Li, and R. McLaren, "Heterogeneous Reactions of Glyoxal on Particulate Matter: Identification of Acetals and Sulfate Esters," *Environmental Science & Technology* 39, no. 6 (2005): 1532–1541, https://doi.org/10.1021/es048375y.

28. F. Aubriet and V. Carré, "Potential of Laser Mass Spectrometry for the Analysis of Environmental Dust Particles—A Review," *Analytica Chimica Acta* 659, no. 1–2 (2010): 34–54, https://doi.org/10.1016/j.aca.2009.11.047.

29. Deposition numbers 2539278 (**4**), and 2547147 (**4′**, R = 4-Me-C_6H_4-CH_2-) contain the supplementary crystallographic data for this paper. These data are provided free of charge by the joint Cambridge Crystallographic Data Centre and Fachinformationszentrum Karlsruhe.

Supporting Information

Additional supporting information can be found online in the Supporting Information section.

Supporting File 1: prep70273-sup-0001-SuppMat.pdf.